CELL CYCLE
2020, VOL. 19, NO. 8, 906–917
https://doi.org/10.1080/15384101.2020.1731649

RESEARCH PAPER

Astrocyte-derived exosomes transfer miR-190b to inhibit oxygen and glucose deprivation-induced autophagy and neuronal apoptosis

Xiaoxi Pei, Yucheng Li, Liangfu Zhu, and Zhilong Zhou

Cerebrovascular Division, Henan Provincial People's Hospital, People's Hospital of Zhengzhou University, School of Clinical Medicine, Henan University, Zhengzhou, Henan, China

ABSTRACT

Our previous work has verified that astrocytes (AS)-derived exosomes (AS-Exo) inhibited autophagy and ameliorated neuronal damage in experimental ischemic stroke. However, the mechanism of AS-Exo regulation of autophagy remains unclear. The aim of this study was to investigate the regulatory mechanism of AS-Exo on neuronal autophagy. The mouse hippocampal neuronal cell line HT-22 was cultured in oxygen and glucose deprivation (OGD) condition to mimic ischemic injury. The primary astrocytes were used to isolate exosomes. Exosome labeling and uptake by HT-22 cells were observed by confocal laser microscopy. miR-190b expression was determined by qRT-PCR. HT-22 cell vitality and apoptosis were determined by CCK-8 assay and TUNEL staining, respectively. Levels of TNF-α, IL-6 and IL-1β were analyzed by ELISA. Protein levels of apoptosis-related cleaved caspase-3, Bax, Bcl-2 and autophagy-related Beclin-1, LC3-I/II, Atg7, P62 were determined by western blot. A dual-luciferase reporter assay was performed to confirm the direct interaction between miR-190b and Atg7. miR-190b expression in AS-Exo was found to be significantly higher than that in AS. AS-Exo-mediated transfer of miR-190b attenuated OGD-induced neuronal apoptosis via suppressing autophagy. Moreover, Atg7 was identified as a target of miR-190b. AS-Exo-mediated transfer of miR-190b regulated autophagy by targeting Atg7. Collectively, our data indicated that AS-Exo transferred miR-190b to inhibit OGD-induced autophagy and neuronal apoptosis.

ARTICLE HISTORY
Received 16 September 2019
Revised 26 November 2019
Accepted 29 December 2019

KEYWORDS
Astrocyte-derived exosomes; miR-190b; autophagy; ischemic stroke

Introduction

Ischemic stroke remains one of the leading causes of morbidity and mortality worldwide [1], which is characterized by acute loss of neurons, astroglia, and oligodendroglia and disruption of synaptic architecture due to cerebral artery occlusion [2]. Despite great improvement in treatment, morbidity and disability of stroke are still high.

Mounting evidence suggests that astrocytes are activated during cerebral ischemia and could secrete exosomes to protect the central nervous system [3–5]. Exosomes are nano-sized membrane vesicles (40–100 nm in diameter) secreted by most cell types [6]. These exosomes have been regarded as a crucial means of intercellular communication by transferring cargos such as lipids, proteins, and microRNAs (miRNAs) [7,8]. For example, astrocytes (AS) secrete exosomes containing miR-19a, which targeted and downregulated expression of phosphatase and tensin homolog (PTEN) in brain metastatic tumor cells, thus promoting brain metastatic outgrowth [9].

Autophagy is a homeostatic, catabolic degradation process whereby cellular proteins and organelles are engulfed by autophagosomes, digested in lysosomes, and recycled to sustain cellular metabolism [10–12]. Evidence suggests that autophagy plays a dual role in the development of cerebral ischemia: On one hand, excessive autophagy promotes cell death and aggravates nerve injury [13]. On the other hand, moderate autophagy can protect cells through removing damaged tissues and proteins. Our previous work has verified that astrocytes-derived exosomes (AS-Exo) inhibited autophagy and ameliorated neuronal damage in experimental ischemic stroke [14]. However, the mechanism of AS-Exo regulation of autophagy remains unclear.

Recently, Jovičić A et al compared miRNA expression in the primary mouse AS and AS-Exo, and found that miR-190b was significantly up-regulated in AS-Exo than that in AS [15]. In this study, we confirm that miR-190b is increased in AS-Exo relative to AS. Furthermore, our bioinformatics analysis revealed

CONTACT Yucheng Li liyuch17@163.com

that autophagy-related gene 7 (Atg7) was a putative target of miR-190b (Targetscan). We further demonstrate that AS-Exo-mediated transfer of miR-190b inhibits the OGD-induced neuronal apoptosis through regulating autophagy via targeting Atg7.

Materials and methods

Primary astrocytes isolation and culture

Astrocytes were isolated from 3- to 4-day-old neonatal mice as previously described [14]. Astrocytes were cultured in neurobasal medium supplemented with 1% penicillin/streptomycin.

Neurons cell culture

The mouse hippocampal neuronal cell line HT-22 (American Type Culture Collection, Rockville, MD) was cultured in DMEM high glucose medium (Sigma-Aldrich, Saint Louis, MO, USA) containing 10% fetal bovine serum (FBS), 50 mg/ml streptomycin, and 50 U/ml penicillin. Cells were maintained at 37°C in atmosphere containing 5% CO_2.

Isolation and characterization of AS-Exo

Exosomes were extracted from the cell culture medium of astrocytes by differential centrifugation. Exosome-depleted FBS (Gibco) was used to culture astrocytes to avert contamination with FBS-derived exosomes. Briefly, the supernatant was collected and further centrifuged at 2, 000 × *g* for 30 min to discard dead cells, 10, 000 × *g* for 30 min to discard cell debris, and 100, 000 × *g* for 4 h at 4°C. The resultant exosome pellets were resuspended in PBS and prepared for subsequent analysis. The isolated exosomes were washed once with PBS and resuspended for further characterization.

The morphologic characteristics of AS-Exo were observed by transmission electron microscopy (TEM). The size distribution of AS-Exo was evaluated by Nanosizer™ technology (Malvern Instruments, Malvern, Worcestershire, UK). The protein levels of exosomal surface markers CD9, CD63 and Alix were examined by western blot.

Cell transfection

The miR-190b mimic, miR-190b inhibitor, corresponding negative controls mimic NC and inhibitor NC, Atg7 overexpression vector, empty vector, siRNAs targeting Atg7 (si-Atg7), and scramble siRNA were purchased from GenePharma (Shanghai, China). Astrocytes or HT-22 cells were transfected with miR-190b mimic and inhibitor or corresponding controls at a final concentration of 50 nM. Atg7 overexpression vector and si-Atg7 were transfected into HT-22 cells. Cell transfection was carried out by using Lipofectamine® 2000 (Invitrogen, Carlsbad, CA, USA). Following transfection for 48 h, cells were harvested for qRT-PCR analysis to examine miR-190b expression.

Quantitative real-time PCR (qRT-PCR)

After treatment, the cells or exosomes were lysed and total RNA was extracted using TRIzol (Invitrogen). After reverse transcription, the expression of miR-190b were using the miRNA qRT-PCR kit (GeneCopoeia) in Applied Biosystems 7500 PCR system (Foster, CA) using specific primers miR-190b-Forward, 5′- CCGGGTGATATGTTTGATATA –3′; and a universal reverse primer, 5′- GTGCAGGG TCCGAGGT –3′ [16]. The expression level of miR-190b was normalized to the relative expression of snRNA RNU6B and was calculated using the $2^{-\Delta\Delta Ct}$ method.

Exosome labeling and uptake

Briefly, 400 μL of DiI was added to the exosome suspension. After incubation for 5 min, an equal volume of exosome-depleted bovine serum albumin was added to stop the reaction. Subsequently, the exosomes were washed twice with PBS to remove any unbound dye. HT-22 cells were incubated with the DiI-labeled or denatured exosomes for 24 h. Then HT-22 cells were fixed in 4% paraformaldehyde and stained with Hoechst 33342. The images were captured using a confocal microscope.

Oxygen and glucose deprivation (OGD) treatment

Cells were converted into an ischemia-mimetic solution–Hanks' solution (140 mM NaCl, 3.5 mM KCl, 0.43 mM KH_2PO_4, 1.25 mM $MgSO_4$, 1.7 mM $CaCl_2$, 5 mM $NaHCO_3$, 20 mM HEPES, pH7.2–7.4) to induce ischemia, after which cells were then cultured in a hypoxic incubator chamber equilibrated with 95% N_2/5% CO_2 at 37°C for 6 h. Cells in the AS-Exo treatment groups were pretreated with 10 μg/mL AS-Exo and cells in the rapamycin treatment groups were pretreated with 2 mM rapamycin in Hanks' solution for 12 h before OGD.

Cell viability assay

Cell viability assay was conducted using the Cell Counting Kit-8 (CCK-8; Dojindo, Kumamoto, Japan). Briefly, HT-22 cells were seeded in the 96-well plates and were treated with AS-Exo (100 μg/mL) or PBS and were then incubated with CCK-8 reagent at 37°C for 3 h. The OD450 values of different treatment groups were measured using a microplate reader (Bio-Rad 680, Hercules, USA).

Enzyme-linked immunosorbent assay (ELISA)

The levels of various cytokines TNF-α, IL-6 and IL-1β in cell supernatant were measured using their commercial ELISA kits (Abcam, Cambridge, UK) according to the manufacturer's protocol.

Western blot

Total protein was extracted from AS-Exo or HT-22 cells using RIPA lysis buffer (Beyotime, Shanghai, China). Briefly, forty micrograms of protein were loaded per lane and separated using 10% SDS-PAGE gel electrophoresis and transferred onto polyvinylidene difluoride membranes. Subsequently, the membranes were incubated with primary antibodies against primary antibodies including CD9 (1:2000; Abcam, Cambridge, UK), CD63 (1:1000; Abcam), Alix (1:1000; Abcam), cleaved caspase-3 (1:1000, Cell Signaling Technology, Beverly, MA, USA), caspase-3 (1:1000, Cell Signaling Technology), Bax (1:1000, Cell Signaling Technology), Bcl-2 (1:1000, Cell Signaling Technology), Beclin-1 (1:200, Santa Cruz Biotechnology), LC3 (1:1000; Santa Cruz Biotechnology), P62 (1:1000; Santa Cruz Biotechnology), and Atg7 (1:1000; Abcam). The membranes were then incubated with the horseradish peroxidase-conjugated secondary antibody (1:2000; Cell Signaling Technology) for 1 h at room temperature. The blots were analyzed using chemiluminescence detection (ECL, Amersham).

Detection of cell apoptosis

Cellular apoptosis the was assessed using a Terminal deoxynucleotidyl transferase dUTP nick end labeling (TUNEL) Apoptosis Assay kit (Beyotime, Shanghai, China) according to the manufacturer's directions. The ratio of TUNEL-positive cells to total neuronal cells indicates the apoptosis index.

Green fluorescent protein (GFP)-LC3 immunofluorescence

After 12 h of OGD treatment, cells were transfected with GFP-LC3 plasmid using Lipofectamine 2000 (Invitrogen) according to the manufacturer's instructions, then LC3 puncta in HT-22 were counted by immunofluorescence under a fluorescence microscope (Nikon Corporation, Tokyo, Japan).

Dual-luciferase reporter assay

A dual-luciferase reporter assay was performed to validate the binding of miR-190b and the 3′-UTR of Atg7. Briefly, 3′-UTR of Atg7 was amplified and then cloned into pmirGLO vector (Promega, USA). For luciferase assay, 293 T cells were seeded in 24-well plates. When it reached to 70% to 80% confluence, cells were cotransfected with wild type (wt) or mutant Atg7 3′UTR luciferase reporter plasmids, together with control mimics or miR-190b mimics (GenePharma, China) by Lipofectamine 2000 (Invitrogen). Twenty-four hours after transfection, firefly and renilla luciferase activities were measured in cell lysates using the dual-luciferase reporter system.

Statistical analysis

All statistical analyses were conducted using SPSS software version 19.0 (IBM, Chicago, IL, USA). Differences between two groups were determined

by Student's t-test in two groups, or ANOVA if more than two groups. The data are presented as mean ± standard deviation (SD). $P < 0.05$ was considered statistically significant.

Results

Identification of AS-Exo

We initially extracted exosomes from cultured astrocytes by ultracentrifugation, and transmission electron microscopy was used to identify the quality of isolated exosomes and a cup-shaped morphology was observed (Figure 1(a)). Data from Nanosight analysis confirmed that the average size of the vesicles isolated from astrocytes was consistent with exosomes in size (Figure 1(b)). Western blot analysis revealed that the extracted vesicles were positive for 3 different exosome markers (CD9, CD63, Alix) (Figure 1(c)), indicating that complete AS-Exos were extracted. Then miR-190b level was determined by qRT-PCR, and miR-190b expression in AS-Exo was found to be significantly higher than that in AS (Figure 1(d)).

AS-Exo-mediated transfer of miR-190b attenuated OGD-induced neuronal apoptosis

To assess whether AS-Exo regulated apoptosis of neurons after OGD *in vitro* via transferring miR-190b, we isolated exosomes from FAM-miR-190b-transfected astrocytes, labeled the resultant exosomes with Dil and then added to HT-22 cells. FAM-miR-190b signals were green and Dil was red. Nuclei were stained with Hoechst 33342 (blue) (Figure 2(a)). qRT-PCR detection showed that expression level of miR-190b in AS-miR-190bI-Exo group was significantly downregulated relative to AS-NCI-Exo group

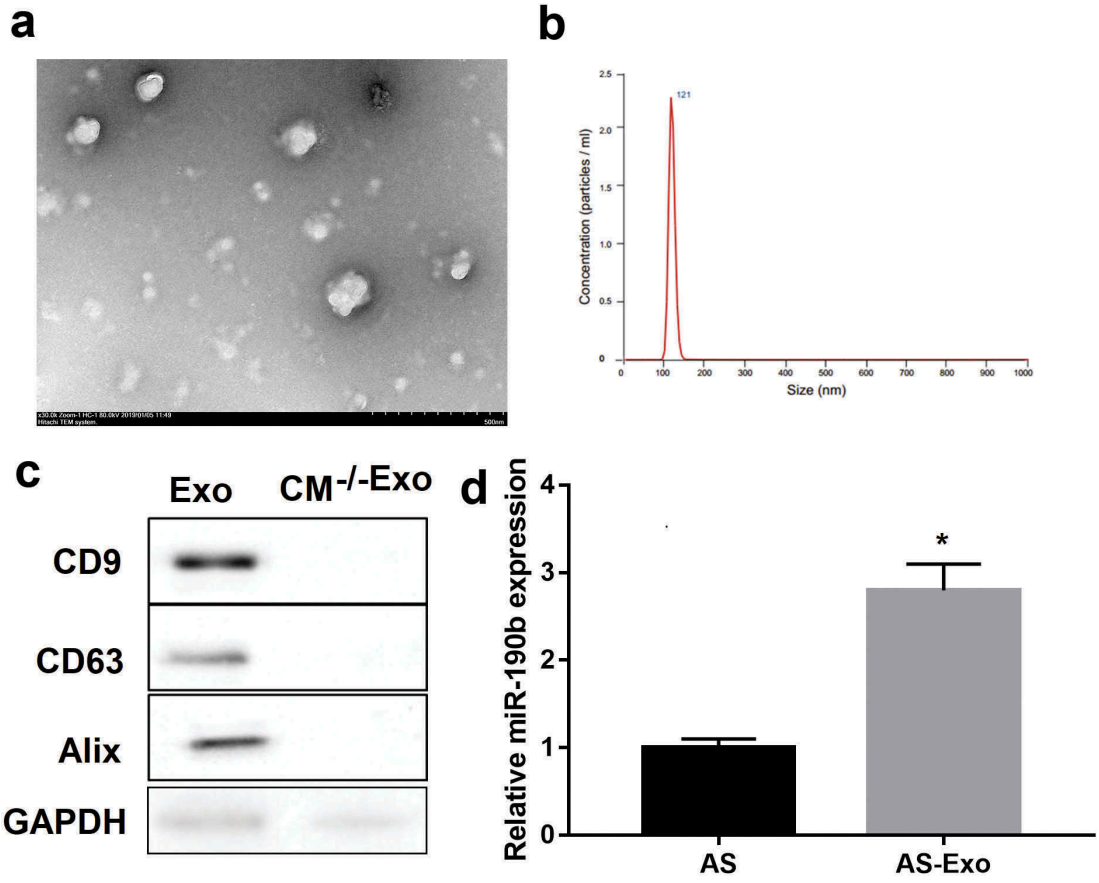

Figure 1. Astrocytes exosomes identification. (a) Exosomes were observed under a transmission electron microscope, characterized as double membrane-bound vesicles. Scale bar = 500 nm.(b) Nanosight results showed that particle size was in the range of 100–150 nm. (c) Expression of the exosome markers CD9, CD63 and Alix confirmed by western blotting. (d) MiR-190b expression in astrocytes (AS) and astrocytes-derived exosomes (AS-Exo) was determined by qRT-PCR. *p < 0.05 versus the AS group. Data are presented as the means ± SD (n = 3).

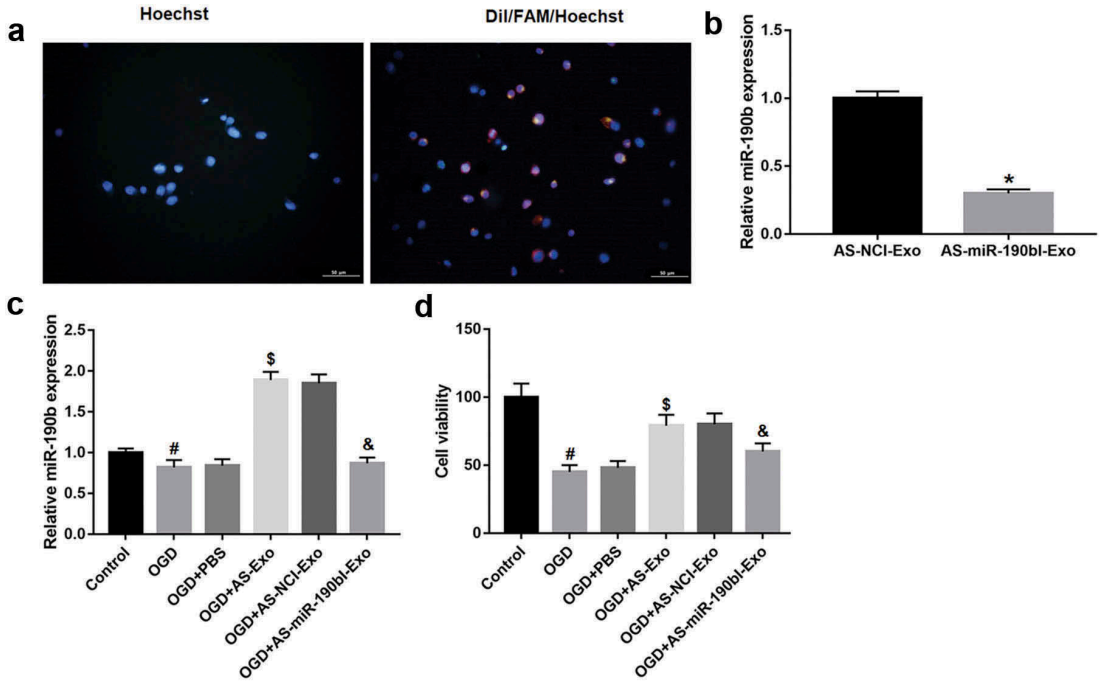

Figure 2. The effect of AS-Exo-mediated transfer of miR-190b on the viability of neurons after OGD. (a) As-Exo transfected with FAM (green)-miR-190b was labeled with DiI (red) and incubated with HT-22 cells (nuclei stained with Hoechst 33342, blue), the distribution and intensity of fluorescence were observed by confocal laser microscopy to analyze exosomes uptake by neurons. (b) Exosomes were extracted from astrocytes after transfection with miRNA inhibitor control (AS-NCI-Exo) and miR-190b inhibitor (AS-miR-190bI-Exo), miR-190b expression in exosomes was detected by qRT-PCR (c-d) HT-22 cells were divided into 6 groups: control group, OGD group, OGD+PBS group, OGD+ AS-Exo group, OGD+ AS-NCI-Exo group and OGD+ AS-miR-190bI-Exo group. (c) MiR-190b expression in HT-22 cells was detected by qRT-PCR. (d) Cell viability in each group was determined by CCK-8 assay. *$p < 0.05$ versus the AS-NCI-Exo group; $^{\#}p < 0.05$ versus the control group; $^{\$}p < 0.05$ versus the OGD+PBS group; $^{\&}p < 0.05$ versus the OGD+AS-NCI-Exo group. Data are presented as the means ± SD (n = 3).

(Figure 2(b)). Next, cultured HT-22 cells were divided into 6 groups according to different treatment: control, OGD, OGD+PBS, OGD+ AS-Exo, OGD+ AS-NCI-Exo, and OGD+ AS-miR-190bI-Exo group. qRT-PCR analysis indicated that miR-190b in HT-22 cells was strongly up-regulated in OGD+ AS-Exo group when compared with OGD+PBS group. Importantly, miR-190b inhibitor attenuated the promoting effect of OGD+ AS-Exo on miR-190b expression (Figure 2(c)). Furthermore, compared with PBS treatment after OGD, AS-Exo treatment after OGD markedly enhanced cell viability. Furthermore, the viability of HT-22 cells in the OGD+ AS-miR-190bI-Exo group was markedly decreased when compared with the OGD+ AS-NCI-Exo group (Figure 2(d)). Moreover, TUNEL staining showed that OGD markedly promoted cell apoptosis in HT-22 cells, AS-Exo significantly repressed apoptosis of OGD-HT-22 cells, and the ability of AS-Exo to repress apoptosis was markedly compromised when miR-190b expression in AS-Exo was inhibited (Figure 3(a)). Consistently. AS-Exo significantly decreased the OGD-induced protein levels of pro-apoptotic cleaved caspase-3 and Bax, whereas increased the OGD-inhibited levels of anti-apoptotic Bcl-2. However, these effects were effectively reversed when miR-190b expression in AS-Exo was inhibited (Figure 3(b)). Moreover, significant reduction of TNF-α, IL-1β and IL-6 were observed in HT-22 cells in the OGD+ AS-Exo group when compared with the OGD+PBS group, but treatment with AS-Exo from miR-190b-downexpressing HT-22 cells after OGD had a significant effect in promoting inflammatory factor expression when compared with OGD+ AS-NCI-Exo group (Figure 3(c–e)). To sum up, these data manifested that AS-Exo-mediated transfer of miR-190b attenuated OGD-induced neuronal apoptosis.

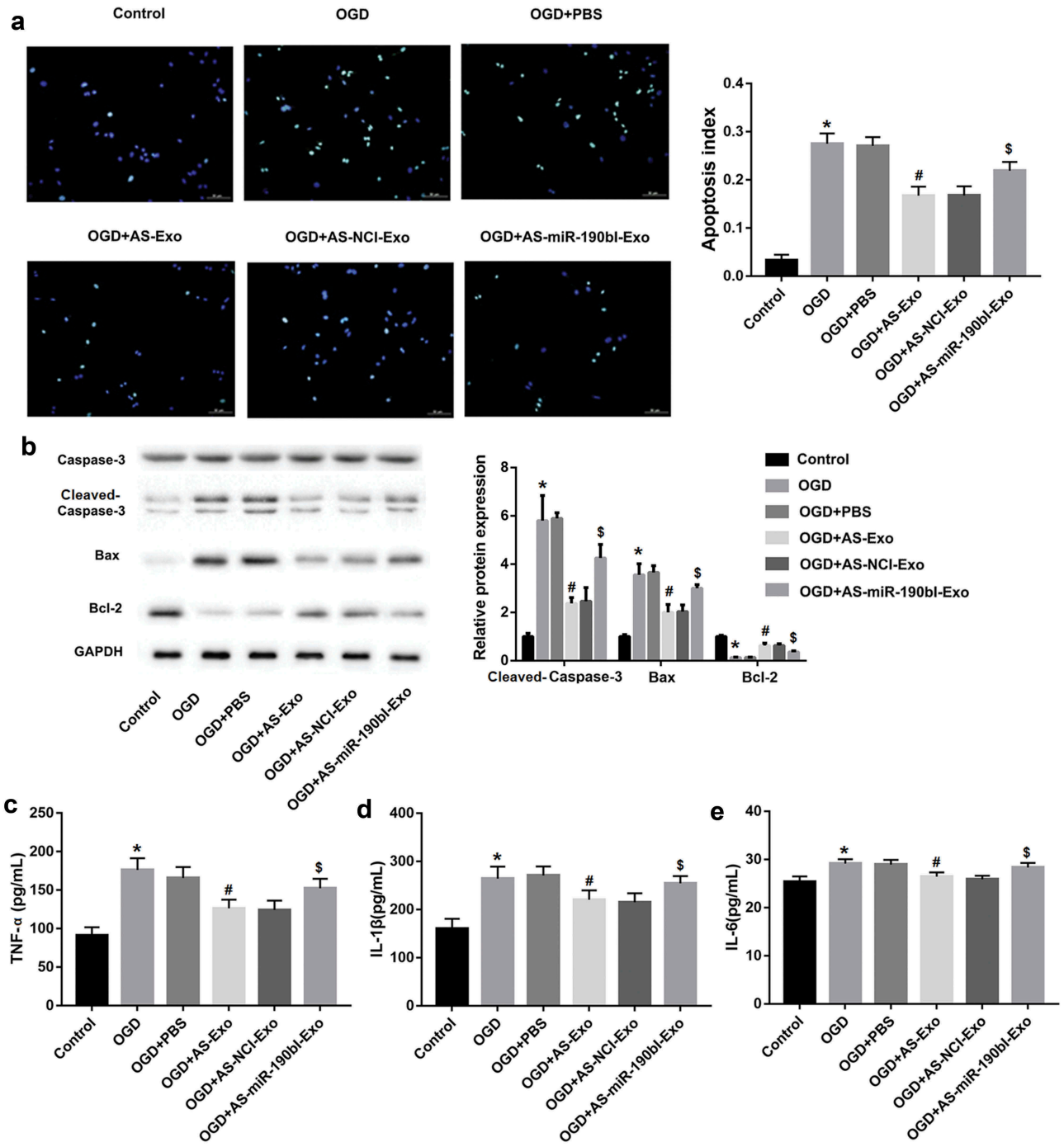

Figure 3. The effect of AS-Exo-mediated transfer of miR-190b on the apoptosis and inflammation of neurons after OGD. HT-22 cells were divided into 6 groups: control group, OGD group, OGD+PBS group, OGD+ AS-Exo group, OGD+ AS-NCI-Exo group and OGD+ AS-miR-190bl-Exo group. (a) Cell apoptosis in each group was determined by TUNEL staining. (b) Relative expression of apoptosis-related protein in HT-22 cells was analyzed by western blot. The levels of TNF-α (c), IL-1β (d) and IL-6 (e) in HT-22 cells were analyzed by ELISA assay. *$p < 0.05$ versus the control group; $^{\#}p < 0.05$ versus the OGD+PBS group; $^{\$}p < 0.05$ versus the OGD+AS-NCI-Exo group. Data are presented as the means ± SD ($n = 3$).

AS-Exo-mediated transfer of miR-190b inhibited OGD-induced neuronal apoptosis via regulating autophagy

To identify whether autophagy was involved in the regulation of AS-Exo-mediated transfer of miR-190b in OGD-induced neuronal apoptosis, cultured HT-22 cells were treated according to the groups: control, OGD, OGD+PBS, OGD+ AS-Exo, OGD+ AS-NCI-Exo and OGD+ AS-miR-190bI-Exo group. Cell autophagy in each group was detected by western blot and GFP-LC3 immunofluorescence assay. Western blot analysis showed that AS-Exo decreased the ratio of LC3-II/LC3-I and the protein levels of Beclin-1 and Atg7, while increased P62 level in OGD-HT-22 cells, but these effects were reversed when the OGD-HT-22 cells were pretreated with miR-190b inhibitor (Figure 4(a)). Consistently, GFP-LC3 immunofluorescence assay indicated that AS-Exo led to a significant decrease in GFP-LC3 puncta in OGD-HT-22 cells, which was rescued by AS-miR-190bI-Exo treatment (Figure 4(b)). To further validate the suppressing effect of miR-190b on HT-22 cell autophagy, HT-22 cells were transfected with miR-190b mimic or control and treated with/without autophagy activator rapamycin under OGD conditions. Compared with mimic NC+rapamycin group, the levels of LC3-II/I ratio, Beclin-1 and Atg7 levels were decreased while P62 level was increased in the miR-190b mimic+rapamycin group as demonstrated by western blot analyses (Figure 4(c)). CCK-8 assay and TUNEL assay results indicated that induction of autophagy by rapamycin significantly inhibited cell activity while facilitated apoptosis in HT-22 cells transfected with miR-190b mimic when compared with DMSO treatment. Furthermore, miR-190 mimic significantly facilitated cell viability and suppressed cell apoptosis and the proliferation-promoting and anti-apoptotic effect of miR-190b mimic was abrogated by the autophagy activator rapamycin (Figure 5(a,b)) but further enhanced by the autophagy inhibitor 3-MA (Figure 7(a,b)). As shown in Figure 5(c), miR-190b mimic suppressed the protein levels of cleaved caspase-3 and Bax, and promoted Bcl-2 expression, but these effects were reversed when the cells were under the pretreatment of rapamycin. Additionally, ELISA results showed that miR-190b mimic caused a significant decrease in levels of pro-inflammatory TNF-α, IL-6 and IL-1β in HT-22 cells when compared with the mimic NC group. In contrast, induction of autophagy by rapamycin prominently increased levels of these inflammatory cytokines cells when compared with DMSO treatment. Of note, the inflammation-inhibitory effect of miR-190b mimic was effectively abrogated by rapamycin (Figure 5(d–f)). Given that, our findings suggested that AS-Exo-mediated transfer of miR-190b inhibited OGD-induced neuronal apoptosis and inflammation via suppressing autophagy.

AS-Exo-mediated transfer of miR-190b regulated autophagy by targeting Atg7

To determine whether the transferred miR-190b, once inside the cells, could bind directly to the 3′-untranslated region (3′-UTR) of the target mRNA, miRNA target gene prediction site TargetScan was used to predict potential targets of miR-190b. Among the candidates, we found a highly conservative and specific combination sequence between miR-190b and Atg7 3′UTR (Figure 6(a)). Our results showed that miR-190b mimic significantly repressed luciferase activity when co-transfected with reporter containing WT Atg7 3′UTR but not MUT Atg7 3′UTR (Figure 6(b)). Further confirmation of the role of Atg7 in regulating autophagy was carried out by overexpressing Atg7 in the HT-22 cells which were incubated with AS-Exo under OGD conditions. As shown in Figure 6(c,d), compared with control, Atg7 overexpression significantly suppressed cell viability while enhanced apoptosis in HT-22 cells incubated with AS-Exo under OGD conditions, moreover, the expression of apoptosis-related proteins showed consistent results with TUNEL assay results of apoptosis (Figure 6(e)). In contrast, Atg7 silencing significantly enhanced cell viability while inhibited apoptosis in HT-22 cells incubated with AS-Exo under OGD conditions (Figure 7(c,d)). Significant induction of IL-1β, IL-6, and TNF-α, were observed in HT-22 cells transfected with Atg7 overexpression after treatment with OGD+ AS-Exo compared with those from vector group (Figure 6(f–h)). The above results indicated that AS-Exo-mediated transfer of miR-190b regulated autophagy by targeting Atg7.

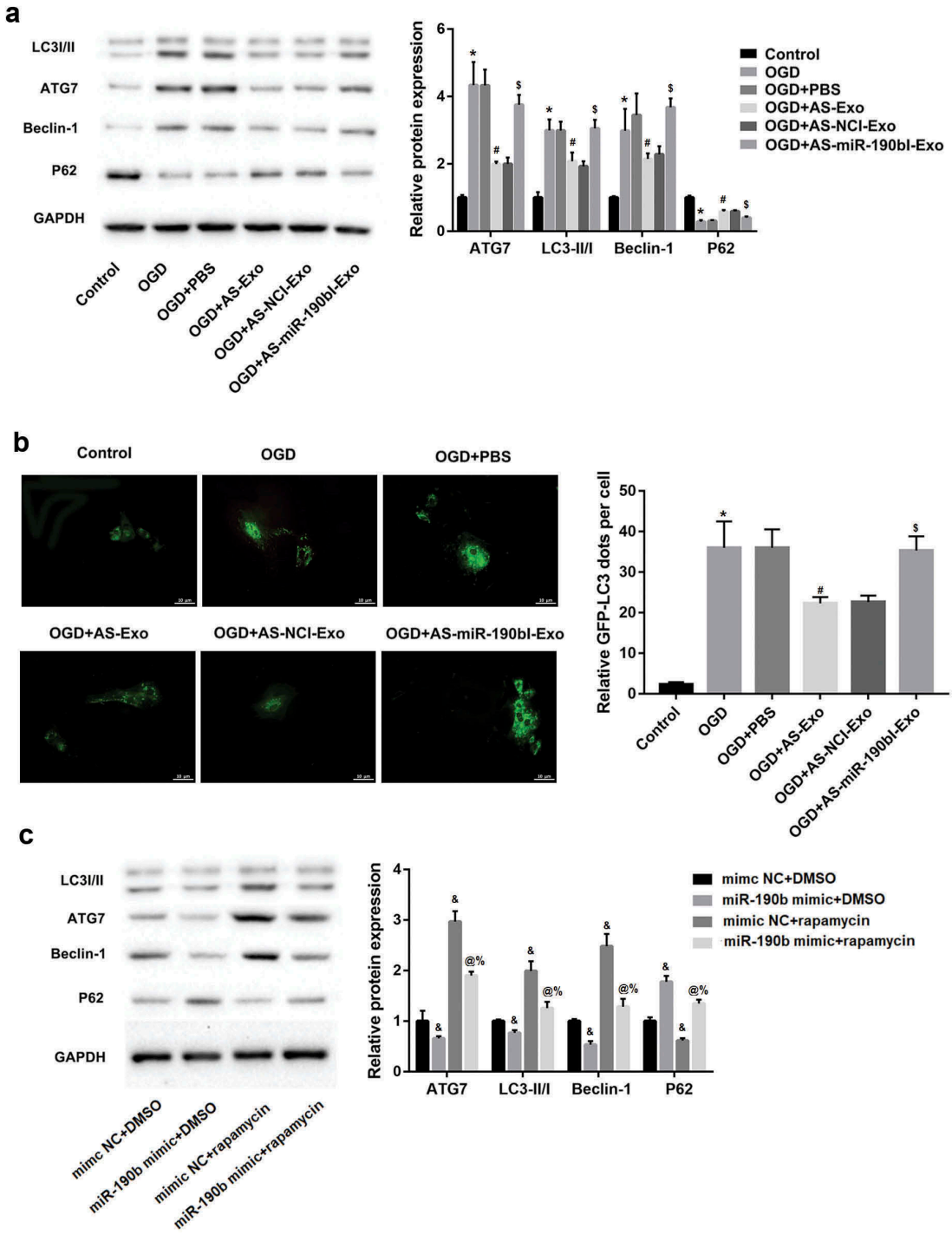

Figure 4. AS-Exo-mediated transfer of miR-190b suppressed autophagy.

HT-22 cells were divided into 6 groups: control group, OGD group, OGD+PBS group, OGD+AS-Exo group, OGD+ AS-NCI-Exo group and OGD+ AS-miR-190bI-Exo group. (a) The protein levels of LC3-I, LC3-II, Atg7, Beclin-1, and P62 in each group were analyzed by western blot. (b) Autophagy vesicles formation in each group was observed by GFP-LC3 immunofluorescence assay. Scale bar: 10 μm. (c) HT-22 cells were transfected with miR-190b mimic or control and treated with/without rapamycin under OGD conditions. The protein expression of LC3-I, LC3-II, Atg7, Beclin-1, and P62 was analyzed by western blot. *$p < 0.05$ versus the control group; $^{\#}p < 0.05$ versus the OGD+PBS group; $^{\$}p < 0.05$ versus the OGD+AS-NCI-Exo group; $^{\&}p < 0.05$ versus the mimic NC+DMSO group, $^{@}p < 0.05$ versus the miR-190b mimic+DMSO group; $^{\%}p < 0.05$ versus the mimic NC+rapamycin group. Data are presented as the means ± SD ($n = 3$).

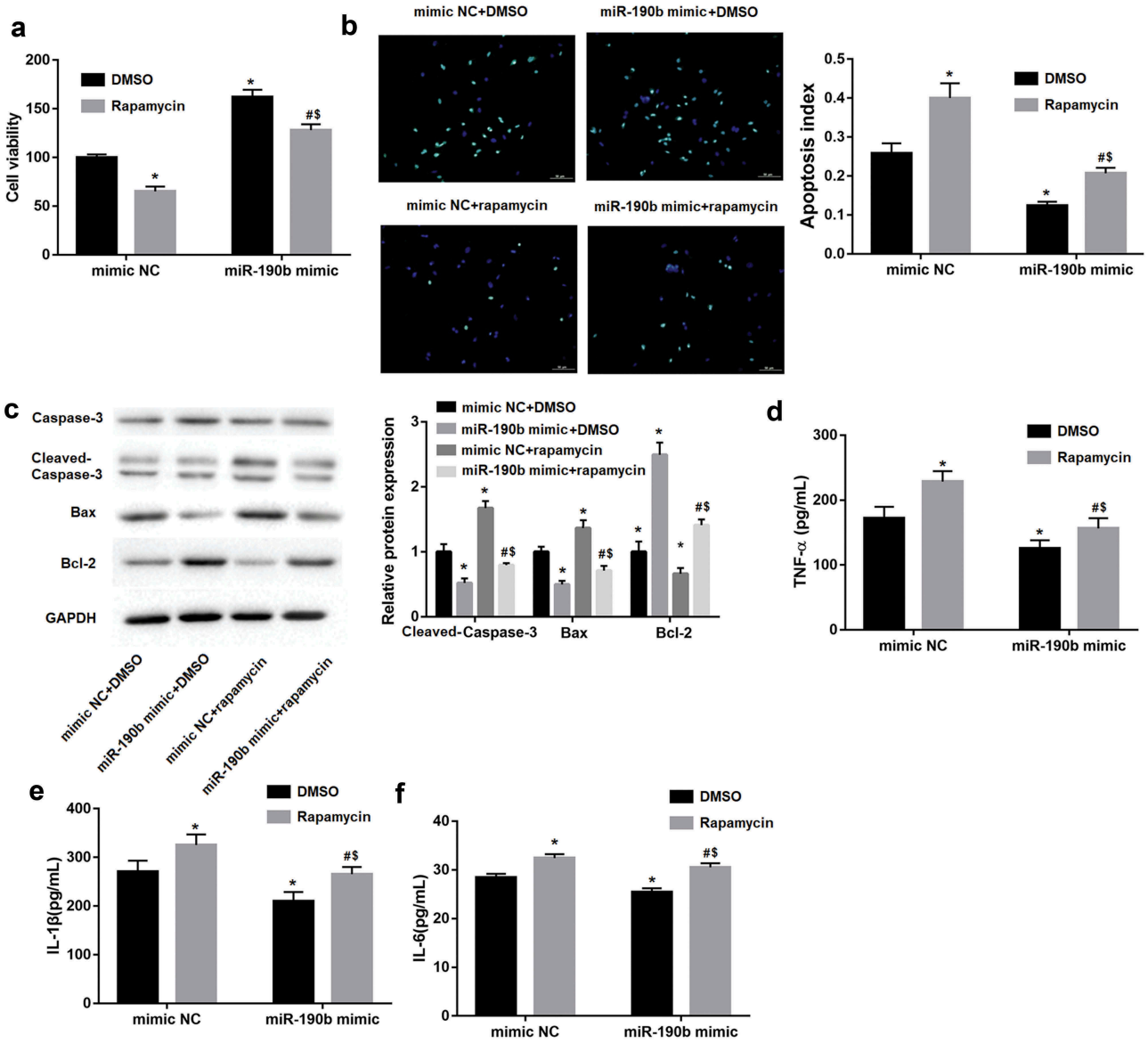

Figure 5. AS-Exo-mediated transfer of miR-190b attenuated OGD-induced neuronal apoptosis and inflammation via regulating autophagy.

HT-22 cells were transfected with miR-190b mimic or control and treated with/without rapamycin under OGD conditions. (a) Cell viability was determined by CCK-8 assay. (b) Cell apoptosis was determined by TUNEL staining. (c) Relative expression of apoptosis-related protein in HT-22 cells was analyzed by western blot. The levels of TNF-α (d), IL-1β (e) and IL-6 (f) in HT-22 cells were analyzed by ELISA assay. *$p < 0.05$ versus the mimic NC+DMSO group; $^{\#}p < 0.05$ versus the miR-190b mimic+DMSO group; $^{\$}p < 0.05$ versus the mimic NC+rapamycin group. Data are presented as the means ± SD (n = 3).

Discussion

In the present study, we initially demonstrated that miR-190b expression in AS-Exo was found to be significantly higher than that in AS. Furthermore, we validated that AS-Exo-mediated transfer of miR-190b inhibited OGD-induced neurons apoptosis via regulating autophagy. Eventually, we identified miR-190b targeting the 3′-UTR region of the neurotropic gene Atg7, and AS-Exo-mediated transfer of miR-190b regulated autophagy by targeting Atg7.

Exosomes act as mediators of cell-cell communication [17–19] and are carriers for functional miRNA delivery [7,20,21]. Exosomes have great promise in clinical applications as biomarkers and/or as potential therapeutic tools [7,22]. Emerging evidence suggests that AS-Exo results in improved survival of neurons under hypoxic and ischemic conditions [5].

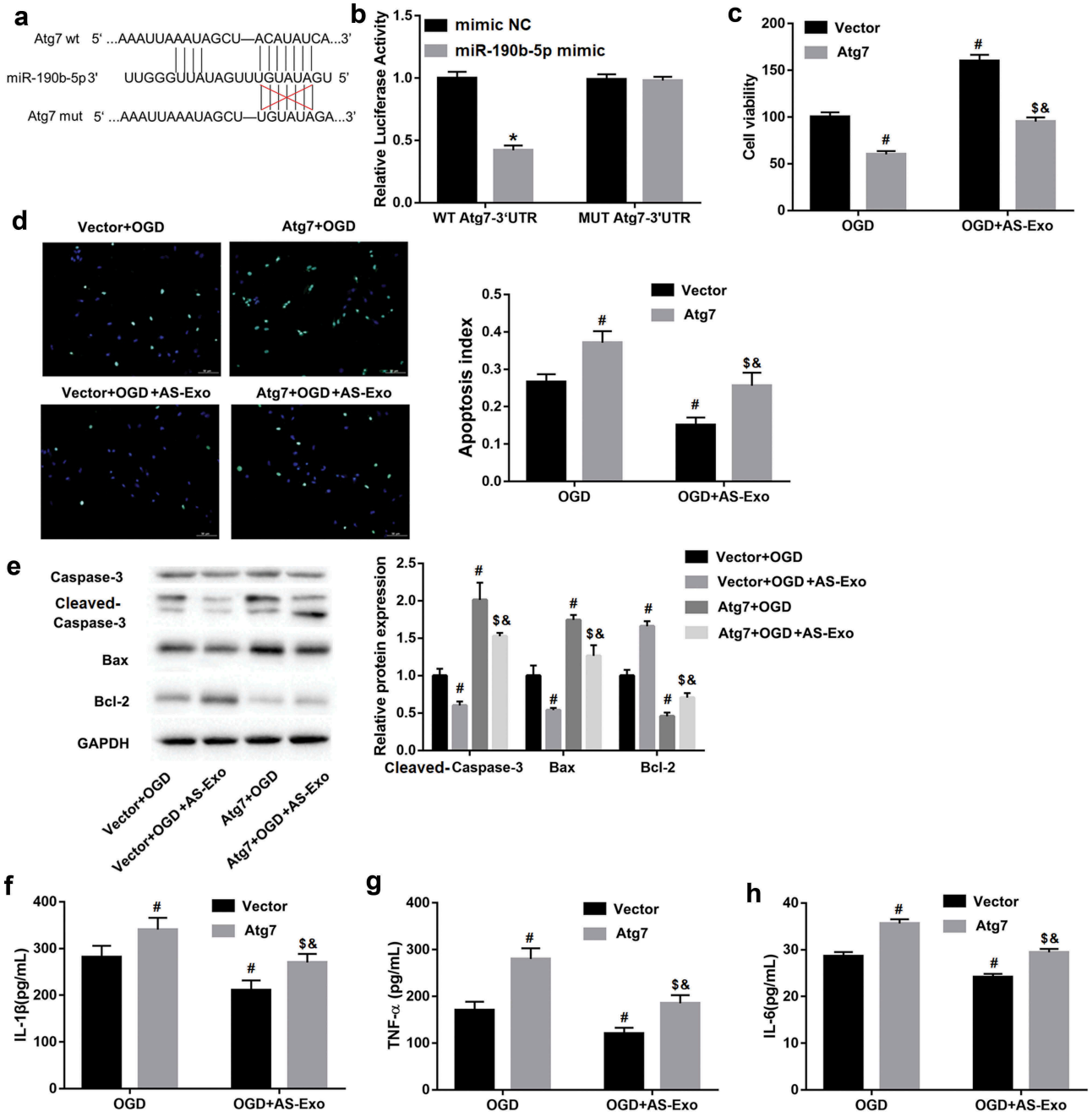

Figure 6. AS-Exo-mediated transfer of miR-190b regulated autophagy by targeting Atg7. (a) Schematic of the putative miR-190b target site in Atg7 3′-UTR and the eleven mutated nucleotides are marked. (b) Luciferase activities were measured using the dual-Luciferase reporter assay. (c-h) HT-22 cells were transfected with Atg7 overexpression vector or control and then incubated with AS-Exo under OGD conditions. (c) Cell viability was determined by CCK-8 assay. (d) Cell apoptosis was determined by TUNEL staining. (e) Relative expression of apoptosis-related protein was analyzed by western blot. Levels of IL-1β (f), TNF-α (g), IL-6 (h) were analyzed by ELISA assay. *$p < 0.05$ versus the mimic NC group; $^{\#}p < 0.05$ versus the Vector+OGD group; $^{\$}p < 0.05$ versus the Vector+OGD+AS-Exo group; $^{\&}p < 0.05$ versus the Atg7+ OGD group. Data are presented as the means ± SD (n = 3).

In this study, we found that the miR-190b level was increased in AS-Exo. When miR-190b expression in AS-Exo was inhibited, the ability of AS-Exo to repress apoptosis was markedly compromised, suggesting that AS-Exo-mediated transfer of miR-190b attenuated OGD-induced neuronal apoptosis.

Autophagy is a homeostatic, catabolic degradation process to specifically degrade aggregated proteins and damaged cellular organelles, which provides cellular quality control and maintains homeostasis [23]. Increasing evidence has highlighted the important role of autophagy in ischemic stroke. Li et al.

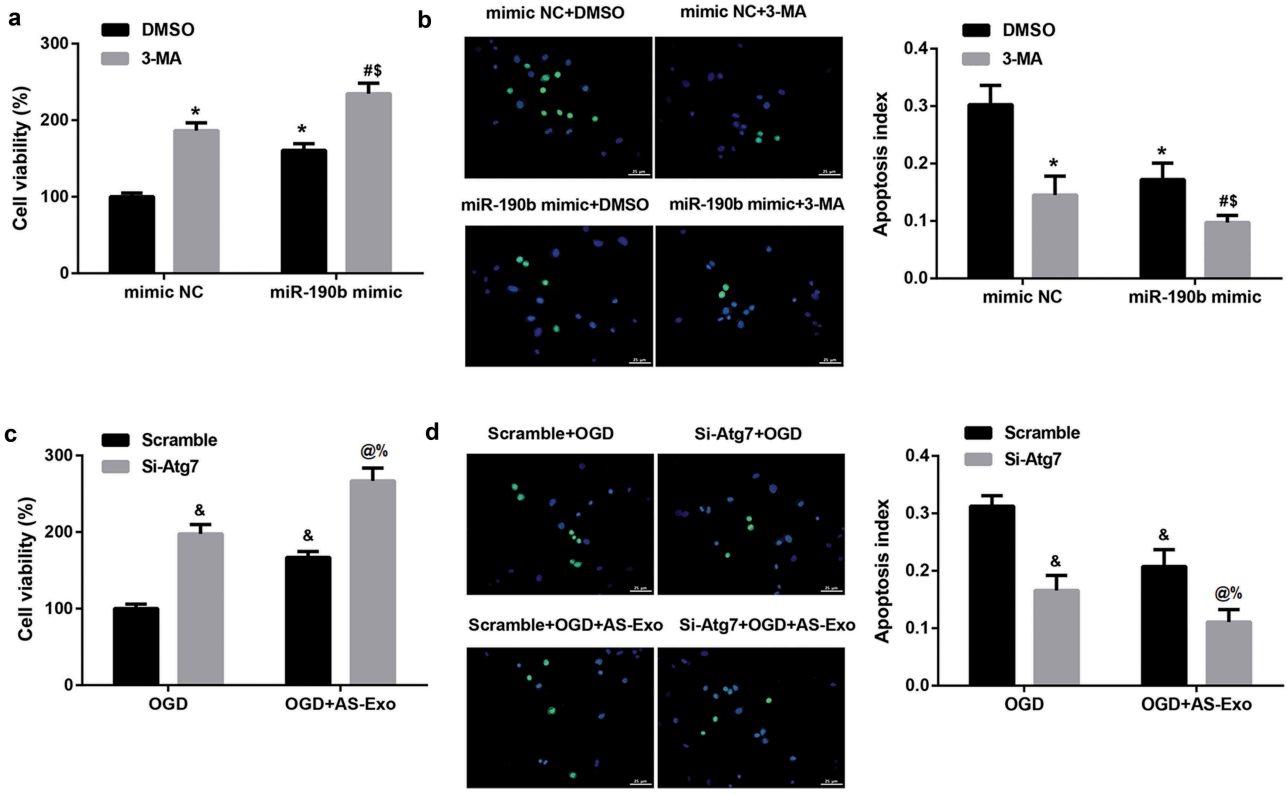

Figure 7. miR-190b promoted cell viability and inhibited cell apoptosis through inhibiting autophagy. (a-b) HT-22 cells were transfected with miR-190b mimic or mimic NC before exposure to 3-MA and OGD treatment. (a) Cell viability was determined by CCK-8 assay. (b) Cell apoptosis was determined by TUNEL staining. (c-d): HT-22 cells were transfected with si-Atg7 or scramble siRNA control before exposure to AS-Exo and OGD treatment. (c) Cell viability was determined by CCK-8 assay. (d) Cell apoptosis was determined by TUNEL staining. *$p < 0.05$ versus the mimic NC+DMSO group; $^{\#}p < 0.05$ versus the mimic NC+3-MA group; $^{\$}p < 0.05$ versus the miR-190b mimic+DMSO group; $^{\&}p < 0.05$ versus the scramble+OGD group; $^{@}p < 0.05$ versus the si-Atg7+ OGD group; $^{\%}p < 0.05$ versus the OGD+AS-Exo+scramble group. Data are presented as the means ± SD (n = 3).

suggested that fingolimod suppressed neuronal autophagy and alleviated ischemic brain damage in mice [24]. Guo D et al. showed that MALAT1 down-regulation attenuated neuronal cell death through inhibiting autophagy in cerebral ischemic stroke [13]. Our previous work has verified that AS-Exo suppressed autophagy and ameliorated neuronal damage in experimental ischemic stroke [14]. In the current study, we demonstrate that AS-Exo-mediated transfer of miR-190b inhibited OGD-induced neuronal apoptosis via regulating autophagy.

Accumulating data have confirmed complex association between autophagy and apoptosis. Caspases can cleave various autophagy-related proteins, and the cleaved fragments generated have different functional activities and cellular localization [25]. A previous study identified that curcumin can inhibit neural stem cell cycle progression from G1 to S, and that these effects are mediated through the regulation of Atg7 [26]. In the present study, miR-190b targeted Atg7, and Atg7 overexpression significantly suppressed the cell viability while enhanced apoptosis in HT-22 cells incubated with AS-Exo under OGD conditions, indicating that AS-Exo-mediated transfer of miR-190b regulated autophagy by targeting Atg7.

In summary, the findings in the present study suggest that the exosomes released from astrocytes suppress neuronal apoptosis. The mechanism of this effect is, at least in part, related to the transfer of miR-190b, which was taken up by neurons, leading to autophagy inhibition. Regulation of miR-190b expression in exosomes released from astrocytes might be a putative therapeutic strategy against the pathogenesis of ischemic stroke.

Disclosure statement

No potential conflict of interest was reported by the authors.

Funding

This study has received funding by The Technology Research Project of Henan Province [No. 142300410404 and No. 122102310076].

References

[1] Xia J, Zhang Y, Zhao H, et al. Non-invasive monitoring of CNS MHC-I molecules in ischemic stroke mice. Theranostics. 2017;7:2837–2848.
[2] Hao L, Zou Z, Tian H, et al. Stem cell-based therapies for ischemic stroke. Biomed Res Int. 2014;2014:468748.
[3] Liu Z, Chopp M. Astrocytes, therapeutic targets for neuroprotection and neurorestoration in ischemic stroke. Prog Neurobiol. 2016;144:103–120.
[4] Shindo A, Maki T, Mandeville ET, et al. Astrocyte-derived pentraxin 3 supports blood-brain barrier integrity under acute phase of stroke. Stroke. 2016;47:1094–1100.
[5] Guitart K, Loers G, Buck F, et al. Improvement of neuronal cell survival by astrocyte-derived exosomes under hypoxic and ischemic conditions depends on prion protein. Glia. 2016;64:896–910.
[6] Mathivanan S, Ji H, Simpson RJ. Exosomes: extracellular organelles important in intercellular communication. J Proteomics. 2010;73:1907–1920.
[7] Zomer A, Vendrig T, Hopmans ES, et al. Exosomes: fit to deliver small RNA. Commun Integr Biol. 2010;3:447–450.
[8] Katakowski M, Buller B, Wang X, et al. Functional microRNA is transferred between glioma cells. Cancer Res. 2010;70:8259–8263.
[9] Zhang L, Zhang S, Yao J, et al. Microenvironment-induced PTEN loss by exosomal microRNA primes brain metastasis outgrowth. Nature. 2015;527:100–104.
[10] Lin L, Rodrigues F, Kary C, et al. Complement-related regulates autophagy in neighboring cells. Cell. 2017;170 (158–71.e8):158–171.e8.
[11] Gottlieb RA, Finley KD, Mentzer RM Jr. Cardioprotection requires taking out the trash. Basic Res Cardiol. 2009;104:169–180.
[12] Ruocco N, Costantini S, Costantini M. Blue-print autophagy: Potential for cancer treatment. Mar Drugs. 2016;14:138.
[13] Guo D, Ma J, Yan L, et al. Down-regulation of lncrna MALAT1 attenuates neuronal cell death through suppressing beclin1-dependent autophagy by regulating Mir-30a in cerebral ischemic stroke. Cell Physiol Biochem. 2017;43:182–194.
[14] Pei X, Li Y, Zhu L, et al. Astrocyte-derived exosomes suppress autophagy and ameliorate neuronal damage in experimental ischemic stroke. Exp Cell Res. 2019;382:111474.
[15] Jovicic A, Gitler AD. Distinct repertoires of microRNAs present in mouse astrocytes compared to astrocyte-secreted exosomes. PloS One. 2017;12:e0171418.
[16] Kang K, Zhang X, Liu H, et al. A novel real-time PCR assay of microRNAs using S-Poly(T), a specific oligo-(dT) reverse transcription primer with excellent sensitivity and specificity. PloS One. 2012;7:e48536.
[17] Rani S, O'Brien K, Kelleher FC, et al. Isolation of exosomes for subsequent mRNA, MicroRNA, and protein profiling. Methods Mol Biol. 2011;784:181–195.
[18] Ahmed KA, Xiang J. Mechanisms of cellular communication through intercellular protein transfer. J Cell Mol Med. 2011;15:1458–1473.
[19] Thery C. Exosomes: secreted vesicles and intercellular communications. F1000 Biol Rep. 2011;3:15.
[20] Pegtel DM, Cosmopoulos K, Thorley-Lawson DA, et al. Functional delivery of viral miRNAs via exosomes. Proc Natl Acad Sci U S A. 2010;107:6328–6333.
[21] Yang M, Chen J, Su F, et al. Microvesicles secreted by macrophages shuttle invasion-potentiating microRNAs into breast cancer cells. Mol Cancer. 2011;10:117.
[22] Bobrie A, Colombo M, Raposo G, et al. Exosome secretion: molecular mechanisms and roles in immune responses. Traffic. 2011;12:1659–1668.
[23] Deng Z, Purtell K, Lachance V, et al. Autophagy receptors and neurodegenerative diseases. Trends Cell Biol. 2017;27:491–504.
[24] Li X, Wang MH, Qin C, et al. Fingolimod suppresses neuronal autophagy through the mTOR/p70S6K pathway and alleviates ischemic brain damage in mice. PLoS One. 2017;12:e0188748.
[25] Ojha R, Ishaq M, Singh SK. Caspase-mediated crosstalk between autophagy and apoptosis: mutual adjustment or matter of dominance. J Cancer Res Ther. 2015;11:514–524.
[26] Wang JL, Wang JJ, Cai ZN, et al. The effect of curcumin on the differentiation, apoptosis and cell cycle of neural stem cells is mediated through inhibiting autophagy by the modulation of Atg7 and p62. Int J Mol Med. 2018;42:2481–2488.